BIOCHEMISTRY
including biophysical chemistry & molecular biology

ARTICLE

pubs.acs.org/biochemistry

Adduction of Cholesterol 5,6-Secosterol Aldehyde to Membrane-Bound Myelin Basic Protein Exposes an Immunodominant Epitope

Natalie K. Cygan,[†] Johanna C. Scheinost,[†] Terry D. Butters,[‡] and Paul Wentworth, Jr.*[,†,§]

[†]The Scripps-Oxford Laboratory and [‡]Oxford Glycobiology Institute, Department of Biochemistry, University of Oxford, South Parks Road, Oxford OX1 3QU, U.K.

[§]Department of Chemistry and The Skaggs Institute for Chemical Biology, The Scripps Research Institute, 10550 North Torrey Pines Road, La Jolla, California 92037, United States

Supporting Information

ABSTRACT: Myelin degradation in the central nervous system (CNS) is a clinical hallmark of multiple sclerosis (MS). A reduction in the net positive charge of myelin basic protein (MBP) via deimination of arginine to citrulline has been shown to correlate strongly with disease severity and has been linked to myelin instability and a defect that precedes neurodegeneration and leads to autoimmune attack. Recently, we have shown that lipid-derived aldehydes, such as cholesterol 5,6-secosterols atheronal A (**1a**) and atheronal B (**1b**), modulate the misfolding of certain proteins such as apolipoprotein B_{100}, β-amyloid, α-synuclein, and κ- and λ-antibody light chains in a process involving adduction of the hydrophobic aldehyde to lysine side chains, resulting in a decrease in the net positive charge of the protein. In this study, we show that the presence of either atheronal A (**1a**) or atheronal B (**1b**) in large unilamellar vesicles (cyt-LUVs) with the lipid composition found in the cytosolic myelin sheath and bovine MBP (bMBP) leads to an atheronal concentration-dependent increase in the surface exposure of the immunodominant epitope (V86−T98) as determined by antibody binding. Other structural changes in bMBP were also observed; specifically, **1a** and **1b** induce a decrease in the surface exposure of L36−P50 relative to control cyt-LUVs as measured both by antibody binding and by a reduction in the level of cathepsin D proteolysis of F42 and F43. Structure−activity relationship studies with analogues of **1a** and **1b** point to the aldehyde moiety of both compounds being critical to their effects on bMBP structure. The atheronals also cause a reduction in the size of the bMBP−cyt-LUV aggregates, as determined by fluorescence microscopy and dynamic light scattering. These results suggest that formation of an imine between inflammatory-derived aldehydes, which effectively reduces the cationic nature of MBP, can lead to structural changes in MBP and a decrease in myelin stability akin to deimination and as such may make a hitherto unknown contribution to the onset and progression of MS.

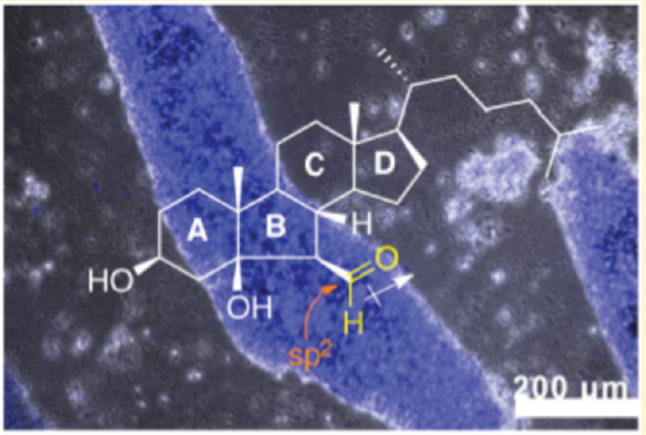

Multiple sclerosis (MS) is an inflammatory demyelinating autoimmune disease characterized by degradation of the central nervous system (CNS) myelin sheath, resulting in chronic and progressive neurological impairment.[1] The classical MS lesions contain T and B lymphocytes and macrophages that are reactive against myelin antigens. The protein responsible for adhesion and stabilization of the intracellular surfaces of compact multilayered myelin is myelin basic protein (MBP) (pI ∼10), which accounts for approximately 30% of the total myelin protein[2−5] (Figure 1A). Structurally, MBP is an 18.5 kDa intrinsically unstructured protein, with its structural orientation being highly dependent on its environment.[6−8] Only subtle changes in the amount or ratio of lipid composition in membranes result in myelin disruption as a result of changes in the electrostatic forces between the negatively charged cytoplasmic membrane surfaces and positively charged MBP.[9]

MBP shows extensive post-translational modification (PTM) with degrees of deimination, phosphorylation, deamidation, methylation, and N-terminal acylation. These modifications give rise to charge variant isoforms C1−C8; C1 is the least modified and most cationic isomer and is the most abundant form of MBP in healthy adult humans. Critically, the least cationic component is C8, with extensive deimination of arginine residues, and its level is elevated in patients with MS, relative to those of age-matched healthy controls.[10,11] Deimination (the conversion of

Received: January 21, 2011
Revised: February 10, 2011
Published: February 11, 2011

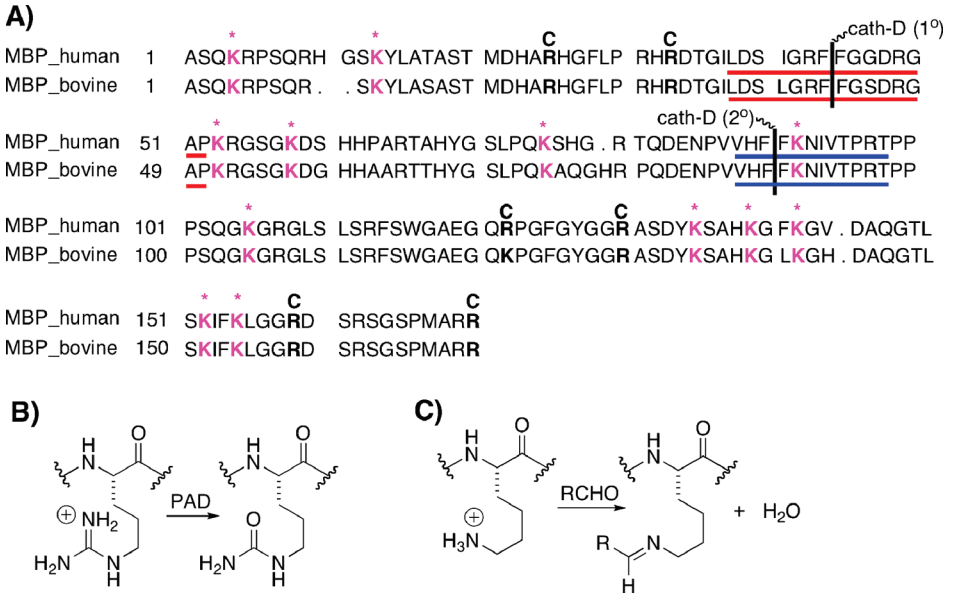

Figure 1. (A) Aligned amino acid sequences of the 18.5 kDa isoforms of human MBP (hMBP, 170 residues) and bovine MBP (bMBP, 168 residues). The number at the beginning of each row refers to the first residue for that sequence. Gaps are marked with periods. In hMBP, R25, R33, R122, R130, R159, and R170 are the sites most often deiminated, giving rise to the C8 isoform, which is the predominant form in MS, and are marked with **C** for citrulline. The lysines throughout hMBP and bMBP that may be valid targets for atheronal adduction are colored pink and marked with asterisks. The blue underlined segment is the major immunodominant epitope of MBP (V86−T98 in the human sequence and V85−T97 in the bovine sequence). The red underlined segment is the MBP cathepsin D (cath-D) binding domain. The primary (1°, F44 and F45 in the human sequence and F42 and F43 in the bovine sequence) and secondary (2°, F89 and F90 in the human sequence and F88 and F89 in the bovine sequence) sites of cleavage of MBP by cathepsin D are marked with a black solid line between the residues where proteolysis occurs. B) Scheme for enzymatic deimination of an arginine residue to citrulline in a peptide. PAD − peptidyl arginine deiminase. C) Schiff base (imine) formation between a lysine residue and an aldehyde RCHO.

positively charged arginine to uncharged citrulline) (Figure 1B) weakens the ability of MBP to cause adhesion of lipid bilayers through electrostatic interactions and has a direct correlation with disease severity.[2,3,5,7,10−20] Using a recombinant murine MBP isoform with R or K (at a locus in the murine sequence that corresponds to R in the human protein) → Q mutations to mimic the citrullination of human MBP, Harauz and co-workers[21] showed that the immunodominant epitope (V83−T92 in the murine sequence) was more solvent-exposed in the maximally deiminated isoform (*rmC8*) than in the least deiminated isoform (*rmC1*). This peptide sequence represents the minimal epitope for T cell recognition of human MBP (V86−T98 in the human sequence) with the highest affinity for MHC class II haplotype, HLA-DR, believed to be associated with an increased risk of MS.[22] Thus, the current thinking in the field is that a reduction in the cationic status of hMBP induces changes in the structure and function of this critical protein that renders it unable to perform its role of compaction and maintenance of the integrity of the myelin sheath and makes it a target for autoimmune attack.[23]

Recently, we have discovered a new class of cholesterol oxidation products termed atheronals **1a** and **1b** in vivo[24,25] (Figure 2). Aldehydes **1a** and **1b** are chemically unique as oxysterols, because the steroid nucleus is disrupted at the C5−C6 bond. Both atheronal A and atheronal B have been isolated from atherosclerotic plaque material;[24] the systemic levels of **1b** are elevated in patients with advanced atherosclerosis, and critically from the perspective of MS, the CNS levels of **1b** are elevated in patients with an inflammatory neurological disease, Lewy body dementia.[26] Thus, both the local and systemic levels of the atheronals are related to the combination of cholesterol levels and inflammatory status.[24,27,28] What makes the atheronals potentially important in the context of this study is the fact that they have been shown to modulate the misfolding of a number of disease-related proteins such as apolipoprotein B_{100},[24] β-amyloid,[29−31] α-synuclein,[26] antibody light chains,[32] and a murine prion protein[33] via a process that involves, in part, adduction to specific lysine side chains in the sequence that yields imines (Schiff bases) (Figure 1C).[30] This process essentially reduces the cationic charge of the protein and elevates the local hydrophobicity of these adducted proteins. These effects combine to either trigger or inhibit misfolding events in susceptible proteins.

Herein, we show that the presence of atheronal A and atheronal B in cyt-LUVs leads to an increase in the surface exposure of the immunodominant epitope (V83−T95 in the bovine sequence) and a decrease in surface exposure of the cathepsin D binding domain (L36−P50 in the bovine sequence) relative to control cyt-LUVs. In addition, the atheronals reduce the size and structural stability of bMBP-induced aggregates. Both these atheronal-induced effects are analogous to those observed with deimination and hint at a potential role for lipid aldehyde-mediated adduction to MBP in the onset and severity of MS.

MATERIALS AND METHODS

Reagents. Bovine myelin basic protein (bMBP) was isolated and purified from bovine brain white matter as previously described.[34] The bMBP used for these studies was >95% pure as measured by analytical high-performance liquid chromatography. Phosphatidylcholine (PC), phosphatidylethanolamine (PE), phosphatidylinositol (PI), and sphingomyelin (sphing)

dx.doi.org/10.1021/bi200109q |*Biochemistry* 2011, 50, 2092–2100

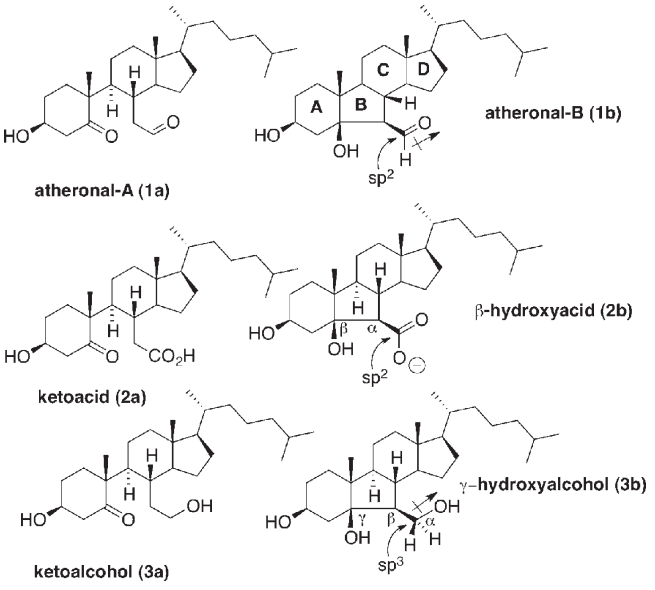

Figure 2. Oxysterols used in this study. Atheronal A (**1a**) and atheronal B (**1b**) contain a reactive aldehyde moiety that comprises an sp^2 carbon with a dipole. The keto acid (**2a**), keto alcohol (**3a**), β-hydroxy acid (**2b**), and γ-hydroxy alcohol (**3b**) are all included as either isosteric ($sp^2 \rightarrow sp^2$), nonisopolar (dipole → anion), or nonisosteric ($sp^2 \rightarrow sp^3$) isopolar (dipole → dipole) analogues of **1a** and **1b**.

were used as supplied by Sigma-Aldrich. Cholesterol (chol) and phosphatidylserine (PS) were supplied by Matraya and were used without further purification. Atheronal A (3β-hydroxy-5-oxo-5,6-secocholestan-6-al) (**1a**), atheronal B (3β-hydroxy-5β-hydroxy-B-norcholestane-6β-carboxaldehyde) (**1b**), keto acid **2a**, and keto alcohol **3a** were synthesized as previously described.[24]

Synthesis of 3β-Hydroxy-5β-hydroxy-B-norcholestane-6β-carboxylic Acid (2b). Acid **2b** was synthesized by adapting a protocol of Smith and Leenay.[35] In brief, aldehyde **1b** (42 mg, 0.1 mmol) was dissolved in tetrahydrofuran (THF) (2.5 mL) containing 2-methyl-2-butene (350 mg, 5 mmol; 2 M solution in THF). The mixture was then treated dropwise with an aqueous solution (1 mL) of 80% sodium chlorite (91 mg, 1 mmol) and monobasic sodium phosphate (84 mg, 0.7 mmol). The reaction mixture was stirred vigorously for 2 h at room temperature, and then the organic solvent was removed in vacuo. The aqueous residue was extracted with ethyl acetate (4 × 10 mL); the combined organic layers were dried with sodium sulfate, and the solvent was evaporated to dryness. The resulting crystals were washed with hexanes to give **2b** as a white solid (38 mg, 87%): ^{1}H NMR (500 MHz, $CDCl_3$) δ 4.05 (m, 1H, H-3), 2.23 (d, 1H, J = 10.0 Hz, H-6), 0.94 (s, 3H, CH_3-19), 0.89 (d, 3H, J = 7.0 Hz, CH_3-21), 0.843 (d, 3H, J = 7.0 Hz, CH_3), 0.839 (d, 3H, J = 7.0 Hz, CH_3), 0.68 (s, 3H, CH_3-18); ^{13}C NMR (125.72 MHz, $CDCl_3$) δ 178.02, 82.95, 67.42, 58.74, 56.66, 55.92, 51.50, 45.56, 44.86, 44.84, 42.85, 39.89, 39.71, 36.44, 35.85, 28.63, 28.44, 28.23, 24.31, 24.07, 23.01, 22.76, 21.72, 18.99, 17.78, 12.73; HR-ESI-MS (ESI+) found 435.3477 $[M + H]^+$, found 457.3288 $[M + Na]^+$, calcd for $C_{27}H_{47}O_4$ 435.3474, calcd for $C_{27}H_{46}O_4Na$ 457.3294.

Synthesis of 3β-Hydroxy-5β-hydroxy-B-norcholestane-6β-hydroxymethyl (3b). Sodium borohydride (38 mg, 1 mmol) was added to a solution of **1b** (42 mg, 0.1 mmol) in methanol (1 mL) and the solution allowed to stir at room temperature for 3 h. The crude material was purified as is by preparative TLC [ethyl acetate/hexane (2:3)], and the desired product eluted from the silica using ethyl acetate. Evaporation of the solvent yielded **3b** as a clear oil (19 mg, 45%): ^{1}H NMR (500 MHz, $CDCl_3$) δ 4.12 (m, 1H, H-3), 3.77 (s, 1H, CH_2-*OH*), 3.66 (dd, 1H, J = 10.0, 10.0 Hz, H_a-7), 3.56 (dd, 1H, J = 10.0, 4.0 Hz, H_b-7), 3.27 (s, 1H, 3β-OH), 2.34 (s, 1H, 5β-OH), 0.92 (s, 3H, CH_3-19), 0.91 (d, 3H, J = 7.0 Hz, CH_3-21), 0.864 (d, 3H, J = 7.0 Hz, CH_3), 0.860 (d, 3H, J = 7.0 Hz, CH_3), 0.65 (s, 3H, CH_3-18); ^{13}C NMR (125.27, $CDCl_3$) δ 84.06, 67.98, 65.10, 56.87, 55.84, 54.72, 50.18, 45.40, 45.23, 44.90, 40.38, 40.16, 39.74, 36.48, 35.86, 28.85, 28.33, 28.24, 26.94, 24.74, 24.06, 23.02, 22.78, 21.66, 19.08, 19.02, 12.76; HR-ESI-MS (ESI$^+$) found 443.3496 $[M + Na]^+$, calcd for $C_{27}H_{48}O_3Na$ 443.3501.

Preparation of Large Unilamellar Vesicles (LUVs). LUVs were prepared as previously described.[13,36] Briefly, aliquots of lipid solutions in chloroform were combined in the desired molar ratio and evaporated in vacuo. LUVs were composed of a lipid mixture similar to that of the cytoplasmic monolayer of myelin (cyt-LUVs) consisting of chol, PE, PS, PC, sphing, and PI in a molar ratio of 44:27:13:11:3:2 and prepared by probe sonication followed by syringe extrusion (Avanti Polar Lipids) through a polycarbonate membrane (100 nm) 14 times.[13,36] cyt-LUVs were prepared in HEPES (20 mM, pH 7.4) containing NaCl (10 mM) for fluorescence microscopy, dynamic light scattering, and flow cytometry experiments and in sodium acetate (50 mM, pH 4.0) containing NaCl (10 mM) for proteolysis with cathepsin D. It should be noted for studies with cyt-LUVs containing oxysterols **1a**−**3b**, the molar percentage of oxysterol replaced an equimolar amount of cholesterol.

Flow Cytometry (FCM). Two loci on the bMBP protein were probed by FCM, the immunodominant epitope (V86−T92 in the bovine sequence) and the primary cathepsin D binding domain (L36−P50 in the bovine sequence). Thus, bMBP was added to 1 mL of cyt-LUVs [20 mM HEPES and 10 mM NaCl (pH 7.4)] (1 mg/mL) containing **1a** and **1b**, **2a** and **2b**, or **3a** and **3b** (0, 10, 20, or 30 μM, equivalent to 0, 0.25, 0.5, or 0.75 mol %, respectively) at a protein:lipid ratio of 1:600. The solution was incubated at room temperature for 30 min to ensure complete aggregation. A murine monoclonal antibody (Abcam, ab22460) that binds specifically to the bMBP immunodominant epitope (V86−T92) or a rat monoclonal antibody (Millipore, MAB395) that binds to L36−P50 of bMBP was then added at a 1:100 dilution and incubated at room temperature for 30 min, followed by incubation with a fluorophore-tagged secondary antibody (Invitrogen, A21202 or A11006) for an additional 30 min at a 1:1000 dilution. Once the primary and secondary antibodies were added to the solution, FACS analysis was performed using a FACScan flow cytometer (Becton and Dickinson) with the threshold set to 900, and the mean fluorescence intensity (MFI) calculated from three collections of 10000 counts. Three separate runs were completed to allow statistical analysis to be performed.

Digestion of Lipid-Associated bMBP with Cathepsin D. Bovine cathepsin D (100 ng, Calbiochem) was added to a suspension of cyt-LUVs (10 μL, 6 mg/mL) containing bMBP at a protein:lipid molar ratio of 1:600 into which had been incorporated **1a** and **1b**, **2a** and **2b**, or **3a** and **3b** (0, 10, 20, or 30 μM, equivalent to 0, 0.25, 0.5, or 0.75 mol %, respectively) in sodium acetate buffer (50 mM, pH 4.0).[21] Each sample was inverted twice and flushed with argon (1 min). Aliquots were taken during the incubation at given times (from 0 to 24 h). The enzymatic reaction was stopped via addition of NuPage LDS

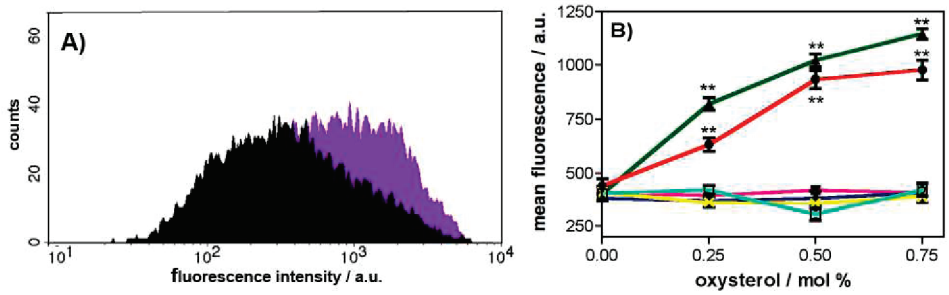

Figure 3. Incorporation of atheronals **1a** and **1b** into cyt-LUVs leads to an increase in surface exposure of the immunodominant epitope (V85−T97) of bMBP. (A) Representative FCM histogram of counts vs log fluorescence intensity for bMBP−cyt-LUV aggregates in the absence (black) or presence of **1a** (0.75 mol %, purple). (B) Graph of MFI ± SD vs [**1a**−**3b**]/mol % measured by flow cytometry (FCM). In a typical experiment, bMBP was added to cyt-LUVs (10 mM) that included 0, 0.25, 0.5, or 0.75 mol % **1a** (▲), **1b** (●), **2a** (◆), **2b** (♦), **3a** (■), or **3b** (×) at a protein:lipid ratio of 1:600. Fluorescence intensity was measured three times (10000 counts each run), and the data are reported as MFI ± standard deviation of three collections of three freshly prepared samples.

loading buffer (4×, 4 μL, Invitrogen) followed by incubation at 110 °C (5 min). The mixture was then resolved by Bis-Tris PAGE (10%) (Invitrogen) and visualized by Coomassie staining. Densitometry was performed for quantitative comparison using a Fuji (Düsseldorf, Germany) LAS1000Pro Intelligent Dark Box II CCD camera, and analyses were conducted using Advanced Image Data Analyzer (AIDA) (Straubenhardt, Germany).

Fluorescence Microscopy of ThT-Treated bMBP−cyt-LUV Aggregates. bMBP was added to cyt-LUVs containing varying amounts of **1a** or **1b** (0, 10, 20, or 30 μM, equivalent to 0, 0.25, 0.5, or 0.75 mol %, respectively) at a protein:lipid molar ratio of 1:600 in aqueous buffer [20 mM HEPES and 10 mM NaCl (pH 7.4)] (50 μL, 6 mg/mL). Thioflavin T (ThT) (50 μM) was added to the solution and the mixture incubated at room temperature for 30 min, after which the solution was transferred to a slide and sealed with a coverslip. The slides were analyzed on a Zeiss Axioplan epifluorescence microscope (Carl Zeiss, Brighton, U.K.), and images were captured using a cooled CCD camera (Carl Zeiss) and metamorph software. Three representative images for each sample were taken.

Dynamic Light Scattering of bMBP−cyt-LUV Aggregates. bMBP−cyt-LUV aggregate size distribution was determined using a Viscotek (Houston, TX) 802 dynamic light scattering (DLS) instrument. bMBP was added to cyt-LUVs (1 mL, 2.5 μM) into which was incorporated **1a** or **1b** (30 μM, 0.75 mol %) of at a 1:600 protein:lipid ratio and the mixture incubated at room temperature for 30 min and then transferred to a quartz cuvette. Scattered light was detected at a 90° angle, and data were obtained from 10 measurements with a 5 s duration and averaged utilizing the instrumental software to determine the aggregate distribution. The average size for each type of aggregate was determined using data collected from three separate runs.

RESULTS

Inclusion of Atheronals (1a and 1b) in cyt-LUVs Increases the Surface Exposure of the Immunodominant Epitope (V86−T98) of bMBP. Flow cytometry (FCM) was used as a minimally disruptive approach for assessing protein domain exposure on the surface of bMBP−cyt-LUV aggregates in the presence or absence of **1a** and **1b**. Thus, to assess whether **1a** or **1b** incorporated into cyt-LUVs affects the surface exposure of the immunodominant epitope (V86−T98) at a protein:lipid ratio found within myelin, an FCM experiment was designed. This FCM approach was considered superior to the more standard ELISA-based experiment for this study because FCM is able to measure antibody binding at regions of bMBP without compromising the integrity of the aggregates by being forced to mount them on a surface such as a microtiter plate. In addition, the threshold of the FACS instrument can be set to measure only large aggregates, ensuring that the measured fluorescence only originates from the primary antibody bound to the immunodominant epitope of fused cyt-LUVs. Prior to in-depth FCM studies, a preliminary analysis that confirmed there were no measurable differences in fluorescence intensity associated with the different cyt-LUV compositions when oxysterols **1a**−**3b** were incorporated was performed. Having thus validated the FCM method for this study, we then measured individual histograms of aggregate count versus fluorescence intensity for formation of a complex of an anti-immunodominant epitope monoclonal antibody with bMBP-loaded cyt-LUVs comprised of increasing amounts (0−0.75 mol %) of each of the series of **1a**−**3b** (Figure 3A). This analysis revealed a concentration-dependent increase in the level of anti-epitope (V86−T98) antibody binding, as measured by fluorescence emission, upon inclusion of the cholesterol 5,6-secosterols **1a** and **1b** into the cyt-LUVs (Figure 3B). Thus, inclusion of 0.75 mol % **1a** or **1b** leads to an ∼3-fold increase in the measured mean fluorescence intensity relative to that of control cyt-LUVs (1023 ± 48 for **1a**, 934 ± 42 for **1b**, and 407 ± 42 for the control). In contrast, there is no significant increase in the mean fluorescence emission relative to that of control cyt-LUVs containing MBP when any of the oxysterol atheronal analogues (**2a**, **2b**, **3a**, and **3b**) are incorporated into LUVs up to the maximal concentration studied, 0.75 mol % (Figure 3B).

Incorporation of Atheronals (1a and 1b) into cyt-LUVs Decreases the Level of Cathepsin D Primary Site (F42 and F43) Proteolysis of bMBP. In our hands, bMBP (∼18.5 kDa) in cyt-LUVs is almost entirely cleaved by cathepsin D at the primary proteolysis site (F42 and F43) after incubation for 24 h in sodium acetate (50 mM, pH 4.0) at 37 °C. This site-specific proteolysis releases a 14.5 kDa protein fragment and can be followed routinely by sodium dodecyl sulfate−polyacrylamide gel electrophoresis (SDS−PAGE) (Figure 4). Inclusion of atheronals **1a** and **1b** in the bMBP-containing cyt-LUVs leads to a concentration-dependent reduction in the extent of the time-dependent cathepsin D-mediated cleavage of bMBP as determined by quantification of the 14.5 kDa band density (Figure 4). Thus,

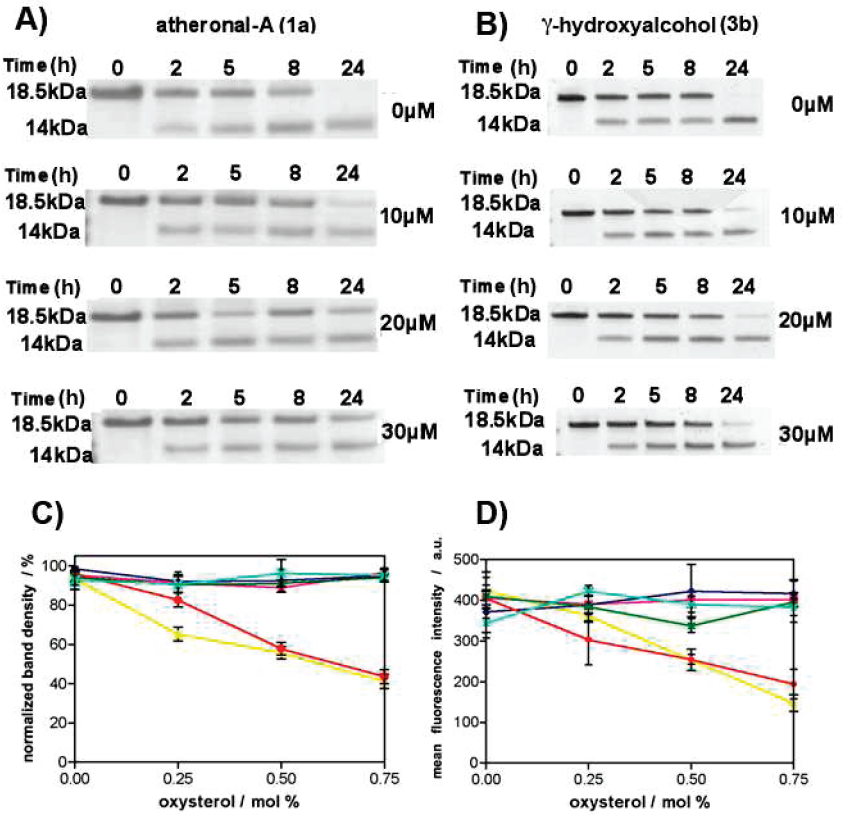

Figure 4. Incorporation of atheronals **1a** and **1b** into cyt-LUVs leads to a decrease in surface exposure of the cathepsin D binding domain (L36−P50) of bMBP. (A) Representative Coomassie-stained SDS−PAGE gels showing time-dependent cathepsin D cleavage of bMBP observed as a loss of the bMBP band at 18.5 kDa and an increase in the magnitude of the band at 14 kDa as a function of atheronal A (**1a**) concentration (0−0.75 mol %). (B) Representative Coomassie-stained gels showing time-dependent cathepsin D cleavage of bMBP observed as a loss of the bMBP band at 18.5 kDa and an increase in the magnitude of the band at 14 kDa as a function of γ-hydroxy alcohol (**3b**) concentration (0−0.75 mol %). (C) Line graph summarizing the cathepsin D (100 ng) digestion of bMBP measured as the mean normalized 18.5 kDa band density as a percentage of the time zero value. In a typical experiment, bMBP was added to cyt-LUVs (10 mM) containing either 0, 10, 20, or 30 μM (0, 0.25, 0.5, or 0.75 mol %, respectively) **1a** (yellow triangles), **1b** (red circles), **2a** (blue diamonds), **2b** (magenta squares), **3a** (light blue times signs), or **3b** (green times signs) at a protein:lipid ratio of 1:600. Data are means ± the standard error of the mean of at least triplicate experiments. (D) Measurement of MFI of the primary cathepsin D binding site (Leu36−Pro50) of bMBP−cyt-LUVs aggregates that contain varying amounts of **1a**−**3b** using FCM. bMBP was added to cyt-LUVs (10 mM) incorporated with either 0, 10, 20, or 30 μM (0, 0.25, 0.5, or 0.75 mol %, respectively) **1a** (yellow triangles), **1b** (red circles), **2a** (blue diamonds), **2b** (magenta squares), **3a** (light blue times signs), or **3b** (green times signs) at a protein:lipid ratio of 1:600. Fluorescence intensity was measured by three collections of 10000 counts, and data are reported as the MFI ± the standard error of the mean of three collections of three separate runs.

with the incorporation of **1a** or **1b** (10 μM, 0.25 mol %) into the cyt-LUVs, there is a decrease in the level of digestion to 65.4 or 80.1%, respectively, of that observed with control cyt-LUVs (Figure 4C). With **1a** or **1b** at 20 μM (0.5 mol %) in the cyt-LUVs, this reduction is 55.8 or 59.4%, respectively, of that of control cyt-LUVs. At the highest concentration of **1a** or **1b** studied (30 μM, 0.75 mol %), the level of proteolysis is 42.1 or 43.2%, respectively, of the control level of cyt-LUV cleavage. In contrast, incorporation of atheronal analogue compounds **2a**−**3b** up to 30 μM into ct-LUVs has no measurable effect on cathepsin D proteolysis of bMBP.

Incorporation of Atheronals (1a and 1b) into cyt-LUVs Decreases the Surface Exposure of L36−P50 Containing the Cathepsin D Primary Cleavage Site (F42 and F43) of bMBP. The primary cathepsin D cleavage site (F42 and F43) is present within the L36−P50 domain for which there is a commercially available rat mAb (MAB395). Thus, the FCM method developed above was modified to measure oxysterol-mediated effects on solvent exposure of the L36−P50 sequence of bMBP (Figure 4D). Inclusion of aldehydes **1a** and **1b** into cyt-LUVs containing MPB resulted in a concentration-dependent reduction in MFI associated with L36−P50 binding of the mAb (MAB395). In contrast, when oxysterol analogues **2a**−**3b** are incorporated into cyt-LUVs, there is no effect on the surface exposure of L36−P50 as measured by FCM.

bMBP−cyt-LUV Aggregates That Contain 1a and 1b Have an Altered Morphology. In general, MBP induces almost instantaneous aggregation of cyt-LUVs to form multilayer aggregates similar to those found in the myelin sheath.[5,37,38] Incorporation of the fluorescent dye thioflavin T and fluorescence microscopy were used to determine the morphological characteristics of these MBP−cyt-LUV aggregates in the presence and absence of aldehydes **1a** and **1b** (Figure 5). Long fibrous aggregates (>1 mm in length) are typically formed when MBP is added to cyt-LUVs and are similar in appearance to those found in the myelin sheath (Figures 5A,E). However, upon addition of increasing concentrations of **1a** or **1b** to the cyt-LUVs, the morphology of the aggregates changes dramatically, becoming less fibrous, smaller, and more spherical in appearance (Figure 5B−D and Figure 5F−H).

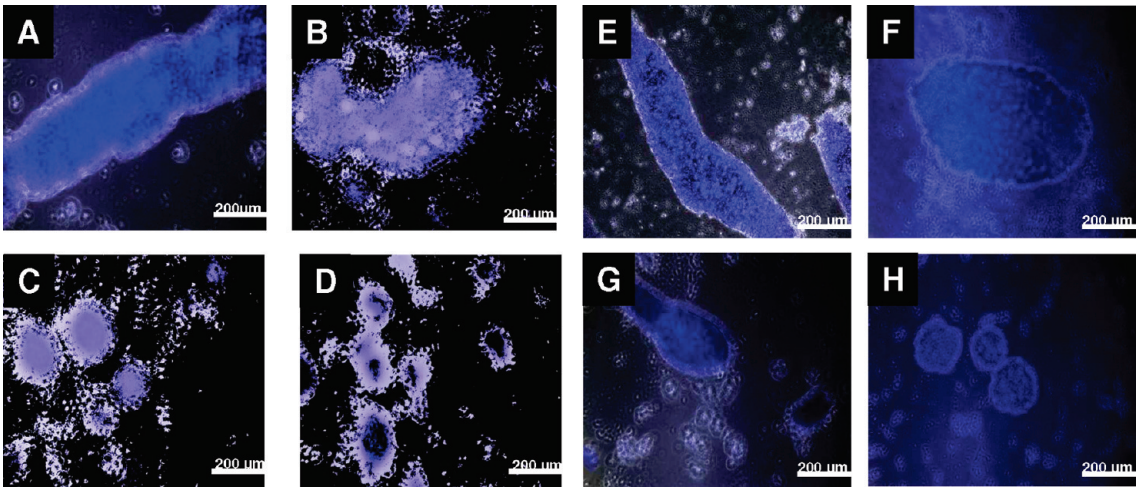

Figure 5. Representative fluorescence microscopy images of bMBP−cyt-LUV aggregates at a protein:lipid molar ratio of 1:600 with varying amounts of **1a** or **1b** incorporated in the LUVs. bMBP was added to cyt-LUVs [20 mM HEPES and 10 mM NaCl (pH 7.4)] (50 μL, 6 mg/mL) containing varying amounts of **1** or **2** (0, 30, 60, or 120 μM) at a protein:lipid molar ratio of 1:600 . Please note **1a** and **1b** were added in place of the corresponding mole percentage of cholesterol. Thioflavin T (ThT) (50 μM) was added to the LUV suspension, which was then allowed to stand for 30 min, added to a viewing slide, dried, and imaged. Long fibrous aggregates are observed in control cyt-LUVs (A and E). When **1a** (B−D) or **1b** (F−H) is incorporated into the cyt-LUVs at 30 μM or 0.75 mol % (B and F), 60 μM or 1.50 mol % (C and G), or 120 μM or 3.00 mol % (D and H), the aggregates adopt a circular appearance with a varying diameter, a clear morphological change relative to the control. Three representative images of each sample were taken.

Table 1. Effect of Atheronals 1a and 1b on the Size Distribution of bMBP−cyt-LUV Aggregates As Measured by DLS[a]

	primary size (nm)	area (%)	secondary size (nm)	area (%)
control	997.46 ± 27.79	96.23 ± 2.05	45.91 ± 10.41	3.76 ± 2.05
1a	431.49 ± 89.93	73.1 ± 12.33	69.15 ± 42.62	25.08 ± 12.01
1b	463.88 ± 53.69	58.90 ± 3.53	126.42 ± 37.76	41.77 ± 4.79

[a] bMBP was added to cyt-LUVs (1 mL, 2.5 mM) in the presence or absence of **1a** or **1b** (30 μM, 0.25 mol %) at a 1:600 protein:lipid molar ratio and the mixture incubated at room temperature for 30 min and then transferred to a quartz cuvette. Scattered light was detected at a 90° angle to incident irradiation, and data were collected from 10 measurements with a 5 s duration and averaged utilizing the instrumental software to determine aggregate distribution. The average size for each type of aggregate was measured using data collected from three separate runs. Data are reported as the mean of two major size distributions (nanometers) with the corresponding area (percentage) ± the standard deviation of three collections of three separate runs.

The bMBP−cyt-LUV Aggregate Size Distribution Is Reduced in the Presence of Oxysterols 1a and 1b. Dynamic light scattering (DLS) was employed to gain quantitative data about the size of the bMBP−cyt-LUV aggregates in the presence and absence of **1a** or **1b**. MBP induces aggregates of cyt-LUVs of one major size (997 ± 28 nm), comprising ∼96% of the total aggregates observed (Table 1). The addition of 30 μM **1a** or **1b** to the cyt-LUVs resulted in a dramatic reduction in aggregate size (431 ± 90 or 464 ± 54 nm, respectively). There was also an increase in the percentage of even smaller aggregates in the oxysterol-incorporated cyt-LUVs [69 ± 43 nm (25% of aggregates, **1a**) or 126 ± 38 nm (∼42% of aggregates, **1b**)].

DISCUSSION

In searching for a potential role for oxysterol aldehyde adduction to CNS proteins and autoimmune pathogenesis, we have extended our studies of cholesterol 5,6-secosterol **1a**- and **1b**-mediated protein misfolding[29−31,33,39] to MBP. As detailed above, it is now clearly established that a reduced cationic nature of MBP, through PTMs such as deimination (R → Q) (Figure 1) and phosphorylation via mitogen-activated protein kinase (MAPK),[40] correlates strongly with the severity of MS.[10,11] At the structural level, it has been shown that this neutralization of the charge of MBP causes significant changes in protein conformation, exposing immunodominant B- and T-cell epitopes,[21,23] renders the protein susceptible to proteolysis,[12,15,41] weakens its ability both to cause adhesion of apposed membranes and to tether the Fyn-SH3 domain to membranes,[42] and even leads to membrane fragmentation.[15−17]

Our group and others have shown that adduction of oxysterols **1a** and **1b** with the primary amine side chain of K residues in peptides and proteins[29,30,32,33] or phosphatidylethanolamine in membrane phospholipids[43,44] involves the formation of a Schiff base, which is a formal neutralization of cationic charge (Figure 1C). Therefore, the question became whether adduction of aldehydes **1a** and **1b** to native MBP in myelin-like membranes in vitro induces similar structural changes in MBP that have been linked to the pathological effects ascribed to PTMs in vivo. The work we report here suggests that the answer to this question is yes. Thus, we have shown that upon replacement of cholesterol with increasing amounts of oxysterols **1a** and **1b** (0.25−0.75 mol %) in bMBP-aggregated cyt-LUVs, used to mimic the cytoplasmic leaflet of the myelin membrane, there is an oxysterol concentration-dependent increase in the liposome membrane surface exposure of the minimal epitope for T-cell recognition of MBP (V86−T98; V85−T97 in the bovine sequence) (Figure 3). This segment of the protein has the highest affinity for the MHC class II haplotype, HLA-DR, believed to be associated with increased susceptibility to MS.[22,45,46] The T- and B-cells found in the CNS of MS patients show specificity for this minimal epitope, and antibodies against it are found in both the brain and spinal fluid of MS patients, emphasizing the humoral and cellular responses to this epitope in disease pathogenesis.[46,47]

A concern when designing this study was being able to assess any potential nonspecific effects on MBP that may result from

substitution of cholesterol in the cyt-LUVs for the more hydrophilic oxysterols **1a** and **1b**. It should be pointed out that substitution of cholesterol was enforced for two reasons, primarily to mimic the in vivo case where we envision cholesterol being oxidized by ROS to form **1a** and **1b**. The second was to maintain a precise MBP:lipid ratio of 1:600 known to ensure complete association between MBP and cyt-LUVs.[21] To help speak to this concern about changing the biophysical characteristics of the LUVs, we also studied a panel of close structural analogues of oxysterols **1a** and **1b** for their effects on MBP orientation in liposomal membranes. From a chemical point of view, there are a number of important features of the analogues. First, ring B of the oxysterols is either open (**2a** and **3a**), to allow mimicry of atheronal A (**1a**), or fused (β-hydroxy acid **2b** and γ-hydroxy alcohol **3b**), to allow mimicry of atheronal B (**1b**). Second, the aldehyde group, essential for Schiff base formation, is replaced with either an isopolar (dipole → dipole) nonisosteric ($sp^2 \rightarrow sp^3$ carbon hybridization) hydroxyl group (**3a** and **3b**) or an isosteric ($sp^2 \rightarrow sp^2$ carbon hybridization) nonisopolar (dipole → anion at pH >5) carboxyl group (**2a** and **2b**) (Figure 2). The essential point was to replace the locus for Schiff base formation with a moiety with a similar charge or shape. Importantly, there was no measurable effect on surface exposure of the immunodominant epitope of MBP when these analogues were incorporated into the cyt-LUVs in the concentration range effective for **1a** and **1b** (0.25−0.75 mol %). This lack of an effect of analogues **2a**−**3b** allows us to conclude with a high degree of certainty that the effect of **1a** and **1b** on MBP conformation in the liposomal membrane must at least in part be due to aldehyde-mediated adduction to K residues in the protein sequence. Another fair conclusion from the study with analogues is that non-aldehyde-containing oxysterols are generally ineffective at mediating changes in MBP orientation within membranes. This is an important observation because, with the exception of **1a** and **1b**, this covers all currently known biologically relevant oxysterols.[48] In general, oxysterols are hydroxylated at various loci around the sterol nucleus or on the alkyl side chain. There are higher-order oxidation products known, such as 7-ketocholesterol, but even this one is largely unreactive with proteins.

Another clear effect of atheronals **1a** and **1b** on MBP conformation in cyt-LUVs is a concentration-dependent reduction in solvent exposure of the primary cathepsin D (EC 3.4.23.5) proteolysis site (F42 and F43 in the bovine sequence) (Figure 4). Cathepsin D cleaves MBP primarily between F42 and F43 and secondarily between F86 and F87 in the immunodominant epitope.[49,50] A single cleavage between F42 and F43 releases a β-peptide ($M_r \sim 14.4$ kDa), in a process that can be followed by quantifying band density via SDS−PAGE. This reduction in the level of cleavage of the F42−F43 bond of MBP in **1a**- and **1b**-containing LUVs was corroborated by a reduction in the level of binding of an anti-L36−P50 rat monoclonal antibody, measured by FCM. These two pieces of data combined point to the fact that this region, L36−P50, is buried to a greater extent in the cyt-LUVs containing **1a** and **1b** than in normal cyt-LUVs. Incorporation of oxysterol analogues **2a**−**3b** had no effect on either cleavage of the F42−F43 bond by cathepsin D or exposure of the L36−P50 domain. A recent study by Harauz and co-workers has shown that a highly citrullinated form of MBP, termed *rm*C8, is cleaved ∼3-fold faster in the F42−F43 site than a native uncitrullinated MBP.[21] Here then is a clear contrast between the effect of citrullination and lipid aldehyde adduction, but one that is not too surprising. MBP is an intrinsically unfolded protein; its orientation and folding to secondary structural elements are highly dependent upon the local environment. Thus, multiple R → Q PTMs cause increased surface exposure of L36−P50, making the protein susceptible to proteolysis by cathepsin D in a process linked to release of the immunodominant epitope V86−T98 (V85−T97 in the bovine sequence) after secondary proteolysis, whereas adduction of atheronal to lysine side chains of MBP buries the L36−P50 site while simultaneously exposing the immunodominant epitope V86−V98 on the surface of the membrane.

Aggregation of cyt-LUVs by bMBP in vitro occurs by charge−charge noncovalent association between one LUV and another. This interaction is due to association between the highly positively charged protein (MBP at +19) and the negatively charged phospholipid headgroups on the solvent-exposed surfaces of the cyt-LUVs. Consequently, long fibrous aggregates (∼1 mm in length) are typically formed, and we have measured these aggregates by both fluorescence microscopy (Figure 5) and dynamic light scattering (DLS) (Table 1). Incorporation of **1a** or **1b** into the cyt-LUVs causes a dramatic reduction in the size and causes a change in the shape of the MBP-induced cyt-LUV aggregates from linear fiber-like to spheres (Figure 5). Clearly, given the importance of charge−charge interactions for stabilizing apposing membranes, atheronal adduction and neutralization of lysine side chain cationic charge may well weaken membrane−membrane interactions and hence not allow large aggregates to form. In addition, an EPR spectroscopy study has shown that the immunodominant epitope region of the protein is highly amphipathic, comprising hydrophobic amino acids on one side and polar amino acids on the other side of an α-helix.[51,52] This segment is generally buried in the lipid bilayer because of a hydrophobic:hydrophilic residue ratio of 13:5 and plays an important role in anchoring the protein in the membrane.[53] Therefore, given that the atheronals cause such a dramatic change in surface exposure of the immunodominant epitope vide supra, this could well weaken the ability of MBP to anchor itself to the lipid membranes and hence cause the observed morphological changes. Furthermore, the structure−activity relationships of compounds **2a**−**3b** when incorporated into cyt-LUVs cause similar morphological changes, showing that the integrity of the myelin is disrupted by the presence of oxysterol compounds not specifically **1a** and **1b**.

Having shown that atheronals **1a** and **1b** in cyt-LUVs can cause such dramatic changes in MBP conformation and function in membranes (exposing the immunodominant epitope V86−T98, burying the L36−P50 domain, and reducing aggregate size in vitro), we now think it is important to consider how this process, lipid aldehyde-induced MBP misfolding, may be relevant in vivo. We have shown that the atheronals are present in all CNS samples, brain and CSF, and their levels are elevated in Lewy body disease, another inflammatory neurological disorder.[26] It is clear that inflammation plays a major role in the pathogenesis of multiple sclerosis.[54] Abundant lipid content and a high level of oxygen consumption make the brain particularly susceptible to free radical-mediated peroxidation and hence lipid aldehyde formation, such as the atheronals.[55,56] In addition, cholesterol is a major lipid component of the myelin, constituting ∼27.7% of total lipid.[56,57] This high level of cholesterol coupled with inflammation and elevated reactive oxygen species (ROS) in MS patients provides an optimal environment for the generation of **1a** and **1b**, so while the actual levels of **1a** and **1b** are not yet known in MS patients, it is certain these reactive aldehydes will be there.

In summary, we have shown that the biologically relevant cholesterol 5,6-secosterol aldehydes, atheronal A (**1a**) and atheronal B (**1b**), cause structural changes in MBP when incorporated into cyt-LUVs that lead to exposure of an immunodominant epitope and cause a reduction in aggregate size and changes in morphology reminiscent of the changes observed in MS. While the in vivo relevance of this process is still to be unraveled, it is clear that this process of adduction of lipid aldehydes to MBP may well be a hitherto unheralded mechanism of autoimmune pathogenesis in MS.

■ ASSOCIATED CONTENT

Supporting Information. DLS data for cyt-LUVs containing oxysterol analogues **2a**−**3b**. This material is available free of charge via the Internet at http://pubs.acs.org.

■ AUTHOR INFORMATION

Corresponding Author

*Telephone: (858) 784-2576. Fax: (858) 784-7385. E-mail: paulw@scripps.edu or paul.wentworth@bioch.ox.ac.uk.

Funding Sources

This work was supported by the National Institutes of Health (AG28300), The Scripps Research Institute (P.W.), and The Skaggs Institute for Chemical Biology (P.W.).

■ ACKNOWLEDGMENT

We thank all members of the Wentworth group (The Scripps Research Institute and The Scripps-Oxford Laboratory) for assistance and suggestions during this work and Mutchmeats Ltd. for providing the bovine brain samples for MBP purification.

■ ABBREVIATIONS

bMBP, bovine myelin basic protein; hMBP, human myelin basic protein; PC, phosphatidylcholine; PE, phosphatidylethanolamine; PS, phosphatidylserine; PI, phosphatidylinositol; sphingo, sphingomyelin; cyt-LUVs, large unilamellar vesicles mimicking the cytoplasmic monolayer of myelin; ThT, thioflavin T; DLS, dynamic light scattering; CNS, central nervous system; THF, tetrahydrofuran.

■ REFERENCES

(1) Boggs, J. M. (2006) Myelin basic protein: A multifunctional protein. *Cell. Mol. Life Sci. 63*, 1945–1961.

(2) Readhead, C., Takasashi, N., Shine, H. D., Saavedra, R., Sidman, R., and Hood, L. (1990) Role of myelin basic protein in the formation of central nervous system myelin. *Ann. N.Y. Acad. Sci. 605*, 280–285.

(3) Omlin, F. X., Webster, H. D., Palkovits, C. G., and Cohen, S. R. (1982) Immunocytochemical localization of basic protein in major dense line regions of central and peripheral myelin. *J. Cell Biol. 95*, 242–248.

(4) Harauz, G., Ishiyama, N., Hill, C. M. D., Bates, I. R., Libich, D. S., and Fares, C. (2004) Myelin basic protein: Diverse conformational states of an intrinsically unstructured protein and its roles in myelin assembly and multiple sclerosis. *Micron 35*, 503–542.

(5) Brady, G. W., Murthy, N. S., Fein, D. B., Wood, D. D., and Moscarello, M. A. (1981) The effect of basic myelin protein on multilayer membrane formation. *Biophys. J. 34*, 345–350.

(6) Tompa, P. (2002) Intrinsically unstructured proteins. *Trends Biochem. Sci. 27*, 527–533.

(7) Bates, I. R., Matharu, P., Ishiyama, N., Rochon, D., Wood, D. D., Polverini, E., Moscarello, M. A., Viner, N. J., and Harauz, G. (2000) Characterization of a recombinant murine 18.5-kDa myelin basic protein. *Protein Expression Purif. 20*, 285–299.

(8) Polverini, E., Fasano, A., Zito, F., Riccio, P., and Cavatorta, P. (1999) Conformation of bovine myelin basic protein purified with bound lipids. *Eur. Biophys. J. 28*, 351–355.

(9) Hu, Y., Doudevski, I., Wood, D., Moscarello, M., Husted, C., Genain, C., Zasadzinski, J. A., and Israelachvili, J. (2004) Synergistic interactions of lipids and myelin basic protein. *Proc. Natl. Acad. Sci. U.S. A. 101*, 13466–13471.

(10) Moscarello, M. A., Wood, D. D., Ackerley, C., and Boulias, C. (1994) Myelin in multiple sclerosis is developmentally immature. *J. Clin. Invest. 94*, 146–154.

(11) Wood, D. D., Bilbao, J. M., O'Connors, P., and Moscarello, M. A. (1996) Acute multiple sclerosis (Marburg type) is associated with developmentally immature myelin basic protein. *Ann. Neurol. 40*, 18–24.

(12) Bates, I. R., Libich, D. S., Wood, D. D., Moscarello, M. A., and Harauz, G. (2002) An Arg/Lys → Gln mutant of recombinant murine myelin basic protein as a mimic of the deiminated form implicated in multiple sclerosis. *Protein Expression Purif. 25*, 330–341.

(13) Boggs, J. M., Yip, P. M., Rangaraj, G., and Jo, E. (1997) Effect of posttranslational modifications to myelin basic protein on its ability to aggregate acidic lipid vesicles. *Biochemistry 36*, 5065–5071.

(14) Wood, D. D., and Moscarello, M. A. (1989) The isolation, characterization, and lipid-aggregating properties of a citrulline containing myelin basic protein. *J. Biol. Chem. 264*, 5121–5127.

(15) Beniac, D. R., Wood, D. D., Palaniyar, N., Ottensmeyer, F. P., Moscarello, M. A., and Harauz, G. (2000) Cryoelectron microscopy of protein-lipid complexes of human myelin basic protein charge isomers differing in degree of citrullination. *J. Struct. Biol. 129*, 80–95.

(16) Boggs, J. M., Rangaraj, G., and Koshy, K. M. (1999) Analysis of the membrane-interacting domains of myelin basic protein by hydrophobic photolabeling. *Biochim. Biophys. Acta 1417*, 254–266.

(17) Shanshiashvili, L. V., Suknidze, N. C., Machaidze, G. G., Mikeladze, D. G., and Ramsden, J. J. (2003) Adhesion and clustering of charge isomers of myelin basic protein at model myelin membranes. *Arch. Biochem. Biophys. 419*, 170–177.

(18) Cheifetz, S., Boggs, J. M., and Moscarello, M. A. (1985) Increase in vesicle permeability mediated by myelin basic protein: Effect of phosphorylation of basic protein. *Biochemistry 24*, 5170–5175.

(19) Cheifetz, S., and Moscarello, M. A. (1985) Effect of bovine basic protein charge microheterogeneity on protein-induced aggregation of unilamellar vesicles containing a mixture of acidic and neutral phospholipids. *Biochemistry 24*, 1909–1914.

(20) MacMillan, S. V., Ishiyama, N., White, G. F., Palaniyar, N., Hallett, F. R., and Harauz, G. (2000) Myelin basic protein component C1 in increasing concentrations can elicit fusion, aggregation, and fragmentation of myelin-like membranes. *Eur. J. Cell Biol. 79*, 327–335.

(21) Musse, A. A., Boggs, J. M., and Harauz, G. (2006) Deimination of membrane-bound myelin basic protein in multiple sclerosis exposes an immunodominant epitope. *Proc. Natl. Acad. Sci. U.S.A. 103*, 4422–4427.

(22) Ota, K., Matsui, M., Milford, E. L., Mackin, G. A., Weiner, H. L., and Hafler, D. A. (1990) T-cell recognition of an immunodominant myelin basic protein epitope in multiple sclerosis. *Nature 346*, 183–187.

(23) Musse, A. A., and Harauz, G. (2007) Molecular 'negativity' may underline multiple sclerosis: Role of the myelin basic protein family in the pathogenesis of MS. *Int. Rev. Neurol. 79*, 149–172.

(24) Wentworth, P., Jr., Nieva, J., Takeuchi, C., Galve, R., Wentworth, A. D., Dilley, R. B., DeLaria, G. A., Saven, A., Babior, B. M., Janda, K. D., Eschenmoser, A., and Lerner, R. A. (2003) Evidence for ozone formation in human atherosclerotic arteries. *Science 302*, 1053–1056.

(25) Wentworth, P., Jr., McDunn, J. E., Wentworth, A. D., Takeuchi, C., Nieva, J., Jones, T., Bautista, C., Ruedi, J. M., Gutierrez, A., Janda, K. D., Babior, B. M., Eschenmoser, A., and Lerner, R. A. (2002) Evidence for antibody-catalyzed ozone formation in bacterial killing and inflammation. *Science 298*, 2195–2199.

(26) Bosco, D. A., Fowler, D. M., Zhang, Q., Nieva, J., Powers, E. T., Wentworth, P., Lerner, R. A., and Kelly, J. W. (2006) Elevated levels of oxidized cholesterol metabolites in Lewy body disease brains accelerate α-synuclein fibrilization. *Nat. Chem. Biol. 2*, 249–253.

(27) Wentworth, P., Jr., Jones, L. H., Wentworth, A. D., Zhu, X., Larsen, N. A., Wilson, I. A., Xu, X., Goddard, W. A., III, Janda, K. D., Eschenmoser, A., and Lerner, R. A. (2001) Antibody catalysis of the oxidation of water. *Science 293*, 1806–1811.

(28) Wentworth, A. D., Jones, L. H., Wentworth, P., Jr., Janda, K. D., and Lerner, R. A. (2000) Antibodies have the intrinsic capacity to destroy antigens. *Proc. Natl. Acad. Sci. U.S.A. 97*, 10930–10935.

(29) Zhang, Q., Powers, E. T., Nieva, J., Huff, M. E., Dendle, M. A., Bieschke, J., Glabe, C. G., Eschenmoser, A., Wentworth, P., Jr., Lerner, R. A., and Kelly, J. W. (2004) Metabolite-initiated protein misfolding may trigger Alzheimer's disease. *Proc. Natl. Acad. Sci. U.S.A. 101*, 4752–4757.

(30) Scheinost, J. C., Wang, H., Boldt, G., Offer, J., and Wentworth, P., Jr. (2008) Cholesterol *seco*-sterol-induced aggregation of methylated amyloid-β peptides: Insights into aldehyde-initiated fibrillization of amyloid-β. *Angew. Chem., Int. Ed. 47*, 3919–3922.

(31) Bieschke, J., Zhang, Q., Powers, E. T., Lerner, R. A., and Kelly, J. W. (2005) Oxidative metabolites accelerate Alzheimer's amyloidogenesis by a two-step mechanism, eliminating the requirement for nucleation. *Biochemistry 44*, 4977–4983.

(32) Nieva, J., Shafton, A., Altobell, L. J., III, Tripuraneni, S., Rogel, J. K., Wentworth, A. D., Lerner, R. A., and Wentworth, P., Jr. (2008) Lipid-derived aldehydes accelerate light chain amyloid and amorphous aggregation. *Biochemistry 47*, 7695–7705.

(33) Scheinost, J. C., Witter, D. P., Boldt, G. E., Offer, J., and Wentworth, P. J. (2009) Cholesterol secosterol adduction inhibits the misfolding of a mutant prion protein fragment that induces neurodegeneration. *Angew. Chem., Int. Ed. 48*, 9469–9472.

(34) Miller, D., and Karpus, W. J. (2007) Experimental autoimmune encephalomyelitis in the mouse. *Curr. Protoc. Immunol.*, 15.11.11–15.11.18.

(35) Smith, A. B., III, and Leenay, T. L. (1989) Indole diterpene synthetic studies. 5. Development of a unified synthetic strategy; a stereocontrolled, second-generation synthesis of (−)-paspaline. *J. Am. Chem. Soc. 111*, 5761–5768.

(36) Inouye, H., and Kirschner, D. A. (1988) Membrane interactions in nerve myelin: II. Determination of surface charge from biochemical data. *Biophys. J. 53*, 247–260.

(37) Lampe, P. D., Wei, G. J., and Nelsestuen, G. L. (1983) Stopped-flow studies of myelin basic protein association with phospholipid vesicles and subsequent vesicle aggregation. *Biochemistry 22*, 1594–1599.

(38) Smith, R. R. (1992) The basic protein of CNS myelin: Its structure and ligand binding. *J. Neurochem. 59*, 1589–1608.

(39) Bieschke, J., Zhang, Q., Bosco, D. A., Lerner, R. A., Powers, E. T., Wentworth, P., Jr., and Kelly, J. W. (2006) Small molecule oxidation products trigger disease-associated protein misfolding. *Acc. Chem. Res. 39*, 611–619.

(40) Erickson, A. K., Payne, D. M., Martino, P. A., Rossomando, A. J., Shabanowitz, J., Weber, M. J., Hunt, D. F., and Sturgill, T. W. (1990) Identification by mass spectrometry of threonine 97 in bovine myelin basic protein as a specific phosphorylation site for mitogen-activated protein kinase. *J. Biol. Chem. 265*, 19728–19735.

(41) Bates, I. R., Boggs, J. M., Feix, J. B., and Harauz, G. (2003) Membrane anchoring and charge effects in the interaction of myelin basic protein with lipid bilayers studied by site-directed spin labeling. *J. Biol. Chem. 278*, 29041–29047.

(42) Homchaudhuri, L., Polverini, E., Gao, W., Harauz, G., and Boggs, J. M. (2009) Influence of membrane surface charge and post-translational modifications to myeline basic protein on its ability to tether the Fyn-SH3 domain to a membrane in vitro. *Biochemistry 48*, 2385–2393.

(43) Bach, D., Wachtel, E., and Miller, I. R. (2009) Kinetics of Schiff base formation between the cholesterol ozonolysis product 3β-hydroxy-5-oxo-5,6-secocholestan-6-al and phsophatidylethanolamine. *Chem. Phys. Lipids 157*, 51–55.

(44) Wachtel, E., Bach, D., Epand, R. F., Tishbee, A., and Epand, R. M. (2006) A product of ozonolysis of cholesterol alters the biophysical properties of phosphatidylethanolamine membranes. *Biochemistry 45*, 1345–1351.

(45) Valli, A., Sette, A., Kappos, L., Oseroff, C., Sidney, J., Miescher, G., Hochberger, M., Albert, E. D., and Adorini, L. (1993) Binding of myelin basic protein peptides to human histocompatibility leukocyte antigen class II molecules and their recognition by T cells from multiple sclerosis patients. *J. Clin. Invest. 91*, 616–628.

(46) Wucherpfennig, K. W., Sette, A., Southwood, S., Oseroff, C., Matsui, M., Strominger, J. L., and Hafler, D. A. (1994) Structural requirements for binding of an immunodominant myelin basic protein peptide to DR2 isotypes and for its recognition by human T cell clones. *J. Exp. Med. 179*, 279–290.

(47) Martino, G., Olsson, T., Fredrikson, S., Hojeberg, B., Kostulas, V., Grimaldi, L. M., and Link, H. (1991) Cells producing antibodies specific for myelin basic protein region 70−89 are predominant in cerebrospinal fluid from patients with multiple sclerosis. *Eur. J. Immunol. 21*, 2971–2976.

(48) Bjorkem, I., and Diczfalusy, U. (2002) Oxsterols: Friends, foes or just fellow passengers?. *Arterioscler., Thromb., Vasc. Biol. 22*, 734–742.

(49) Cao, L., Goodin, R., Wood, D., Moscarello, M. A., and Whitaker, J. N. (1999) Rapid release and unusual stability of immunodominant peptide 45−89 from citrullinated myelin basic protein. *Biochemistry 38*, 5374–5381.

(50) Pritzker, L. B., Joshi, S., Gowan, J. J., Harauz, G., and Moscarello, M. A. (2000) Deimination of myelin basic protein. 1. Effect of deimination of arginyl residues of myelin basic protein on its structure and susceptibility to digestion by cathepsin D. *Biochemistry 39*, 5374–5381.

(51) Mendz, G. L., Brown, L. R., and Martenson, R. E. (1990) Interactions of myelin basic protein with mixed dodecylphosphocholine/palmitoyllysophosphatidic acid micelles. *Biochemistry 29*, 2304–2311.

(52) Warren, K. G., Catz, I., and Steinman, L. (1995) Fine specificity of the antibody response to myelin basic protein in the central nervous system in multiple sclerosis: The minimal B-cell epitope and a model of its features. *Proc. Natl. Acad. Sci. U.S.A. 92*, 11061–11065.

(53) Kitamura, A., Kiyota, T., Tomohiro, M., Umeda, A., Lee, S., Inoue, T., and Sugihara, G. (1999) Morphological behavior of acidic and neutral liposomes induced by basic amphiphilic α-helical peptides with systematically varied hydrophobic-hydrophilic balance. *Biophys. J. 76*, 1457–1468.

(54) Martino, G., Adorini, L., Rieckmann, P., Hillert, J., Kallmann, B., Comi, G., and Filippi, M. (2002) Inflammation in multiple sclerosis: The good, the bad, and the complex. *Lancet Neurol. 1*, 499–509.

(55) Bongarzone, E. R., Soto, E. F., and Pasquini, J. M. (1995) Oxidative damage to proteins and lipids of CNS myelin produced by in vitro generated reactive oxygen species. *J. Neurosci. Res. 65*, 1342–1347.

(56) Smith, K. J., Kapoor, R., and Felts, P. A. (1999) Demyelination: The role of reactive oxygen and nitrogen species. *Brain Pathol. 9*, 69–92.

(57) Saher, G., Brugger, B., Lappe-Siefke, C., Mobius, W., Tozawa, R.-I., Wehr, M. C., Wieland, F., Ishibashi, S., and Nave, K.-A. (2005) High cholesterol level is essential for myelin membrane growth. *Nat. Neurosci. 8*, 468–475.